

Coherence thermometry using multipartite quantum systems

Pranav Perumalsamy^a, Abhijit Mandal ^b, Sovik Roy ^{c,*}, Md Manirul Ali ^d

^aDepartment of Artificial Intelligence and Data Sciences, Chennai Institute of Technology, Chennai 600069, India

^bDepartment of Mathematics, Techno Main Salt Lake, Techno India Group, EM 4/1, Sector V, Salt Lake, Kolkata 700091, India

^cDepartment of Mathematics, Techno Main Salt Lake, Techno India Group, EM 4/1, Sector V, Salt Lake, Kolkata 700091, India

^dCentre for Quantum Science and Technology, Chennai Institute of Technology, Chennai 600069, India

Abstract

We investigate, how finite temperature influences quantum coherence in multipartite open systems by analyzing a tripartite spin boson model subjected to non-Markovian dephasing. Two distinct environmental configurations are considered viz. independent local reservoir and a common structured reservoir characterized by an Ohmic spectral density. In this framework, temperature enters explicitly through the time dependent dephasing rates, enabling a systematic exploration of thermal effects on coherence dynamics. Using the relative entropy of coherence, we examine representative pure states belonging to inequivalent entanglement classes along with physically relevant mixed states constructed from them. Under local non-Markovian dephasing, all states exhibit monotonic coherence decay, with temperature acting as a universal accelerator of decoherence. In contrast, the common reservoir scenario reveals a strikingly non-universal behaviour. While *GHZ* and *Star* type states undergo temperature enhanced degradation, *W* class states and certain Werner type mixtures display robust stationary coherence that remains largely insensitive to thermal fluctuations. These results demonstrate that the thermal susceptibility of coherence is governed not only by environmental configuration but also by the internal architecture of multipartite quantum states. The interplay between reservoir structure and state geometry leads to qualitatively distinct dynamical regimes ranging from rapid thermal fragility to temperature resilient coherence preservation. Our findings identify coherence dynamics as a sensitive probe of structured finite temperature environments and suggest a pathway toward coherence based quantum thermometry and nanoscale calorimetry using engineered multipartite states.

Keywords: quantum thermometry, relative entropy of coherence, open quantum system, multipartite quantum states

1. Introduction

The practical realization of quantum technologies, including computation, communication, and sensing, is critically based on the preservation of quantum coherence, which forms the foundation of quantum superposition and serves as a fundamental resource that allows entanglement and other nonclassical correlations essential for quantum information processing tasks [1, 2, 3, 4, 5, 6, 7]. However, in realistic scenarios, quantum systems inevitably interact with their surrounding environments, leading to decoherence, a detrimental process that progressively destroys quantum coherence and thereby hinders the stable implementation of quantum devices [8, 9, 10, 11]. This environmental interaction consequently compromises the operational viability of quantum states for information processing tasks, including quantum teleportation, quantum

*Corresponding author

Email addresses: pranavpp747@gmail.com (Pranav Perumalsamy), a.mandal1.tmsl@ticcollege.org (Abhijit Mandal )
s.roy2.tmsl@ticcollege.org (Sovik Roy )
manirul@citchennai.net (Md Manirul Ali )

cryptography and many such. In particular, the presence of noise degrades both the quality of the quantum channel and the fidelity of the transmitted state, thereby reducing the overall performance and reliability of protocols such as quantum state teleportation [12, 13, 14, 15, 16]. Thus, the formulation of robust mechanisms to mitigate decoherence and preserve both coherence and entanglement remains a central challenge for realizing reliable and high-fidelity quantum information processing.

In realistic physical scenarios, quantum systems are treated as open quantum systems, where their dynamics are governed by nonunitary evolution due to interactions with external environments. We consider environment-induced decoherence of three qubits under non-Markovian local and common dephasing noise [17, 18, 19, 20]. The quantum master equations employed in our study describe the system's dynamics without relying on the Markovian assumption, namely, the approximation that the environment possesses a negligibly short memory time, often represented through a delta-correlated noise function [21, 22, 23]. This is particularly significant in light of the fact that numerous modern quantum platforms display strong non-Markovian (memory) effects, for which the conventional Markov approximation is inadequate [24, 25]. Such memory effects play important role in a wide range of physical implementations, including photonic and solid-state qubits, hybrid quantum architectures, quantum biological systems, and quantum transport setups. In such settings, non-Markovian dynamics [24, 25, 26, 27, 28, 29, 30] display behaviour that contrasts sharply with the straightforward memoryless evolution characteristic of a Markovian environment. Specifically, the system's time evolution is no longer independent of its past but is instead significantly influenced by the history retained within the reservoir. This, in turn, creates new opportunities for precise experimental engineering of system-environment interactions and tailoring of reservoir spectral characteristics. By deliberately harnessing memory-induced effects, one can reduce the adverse influence of environmental noise and enhance the robustness of quantum coherence [31, 32, 33, 34, 35, 36, 37, 38].

Beyond its detrimental role in accelerating decoherence, environmental temperature can also serve as a physically meaningful control parameter and a metrological resource. In finite-temperature open quantum systems, the dephasing rates explicitly depend on thermal factors appearing in the time-dependent coefficients of the non-Markovian master equation. This intrinsic temperature dependence establishes a direct and quantitative connection between coherence dynamics and the temperature of the thermal environment. As a consequence, the time-resolved decay profile of quantum coherence can be harnessed for quantum thermometry, wherein temperature is inferred from experimentally accessible coherence observables. In multipartite systems, different state architectures exhibit distinct thermal susceptibilities, leading to state dependent amplification or suppression of temperature induced effects. Such behaviour is particularly relevant for quantum calorimetry, where engineered quantum systems act as sensitive probes of energy exchange and heat fluctuations at the quantum scale. From this perspective, understanding how coherence responds to thermal variations is not only crucial for mitigating decoherence but also opens the possibility of employing coherence itself as an operational thermometer in structured non-Markovian environments [39, 40, 41, 42, 43, 44]. Although numerous studies have examined the dependence of quantum coherence and correlations on system-environment configurations, the specific influence of environmental temperature has not yet been explored in a systematic and comprehensive manner. Given that temperature is an omnipresent and often only partially controllable parameter in realistic experimental platforms, a thorough understanding of its role in coherence dynamics is essential. Thermal fluctuations associated with finite temperature reservoirs generally accelerate decoherence; however, the resulting susceptibility is highly state dependent and exhibits nontrivial behaviour, especially in non-Markovian regimes where memory effects can modify or even transiently counteract thermal degradation.

Our analysis focuses on a representative ensemble of tripartite pure states, such as GHZ , W , $W\bar{W}$ and $Star$ states, chosen for their diverse initial coherence and entanglement structures. In this work, we have also considered some mixed states derived from these pure states. By comparing their coherence decay across a temperature gradient, we aim to elucidate the differential sensitivity of various state architectures to thermal noise. The outcomes of this study offer critical insights into the robustness of distinct tripartite states under realistic, finite temperature conditions, thereby informing the optimization of state selection and the devel-

opment of environment engineering strategies for the protection of quantum coherence in practical quantum information processing applications.

The paper is organized as follows: Sec. 2 presents the open quantum system model, discussing the Hamiltonian of three qubits exposed to either local or common dephasing environments. In Sec. 3, we have described the results and discussion part for both pure and mixed three-qubit states evolving under a non-Markovian environment. Sec. 4 concludes the paper with possible future research directions.

2. Description of the models

We discuss the three-qubit models subjected to two types of noisy environments, namely (i) Local Dephasing Environment (LDE) and (ii) Common Dephasing Environment (CDE), as illustrated in Fig. 1.

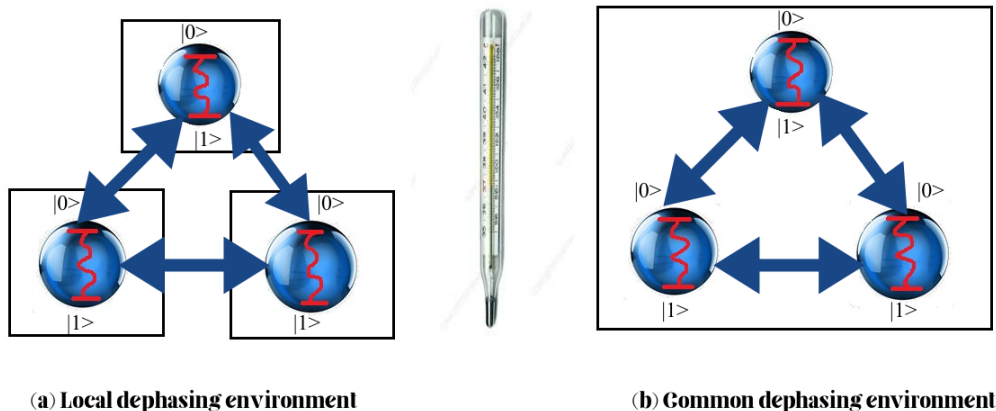


Figure 1: Schematic illustration of a tripartite qubit system subjected to (a) local dephasing and (b) common dephasing environments. In the local configuration, each qubit interacts independently with its own bosonic bath (represented by three squares in fig. (a)) while the spheres are representing the qubits, leading to uncorrelated dephasing. In contrast, in the common environment, all qubits are collectively coupled to a single bosonic reservoir (single square in fig. (b)), giving rise to correlated dephasing dynamics. In both cases, the environments are assumed to be at finite temperature.

2.1. Three Qubits Under Local Dephasing Environment

We consider a spin-boson framework consisting of three non-interacting qubits, each coupled to its own local bosonic environment, as shown in Fig. 1. The total Hamiltonian for the three qubits and their environment is

$$H = \sum_{i=1}^3 \left[\frac{\hbar}{2} \omega_0^i \sigma_z^i + \sum_k \hbar \omega_{ik} b_{ik}^\dagger b_{ik} + \sigma_z^i (B_i + B_i^\dagger) \right], \quad (1)$$

where $B_i = \hbar \sum_k g_{ik} b_{ik}$. In this model, σ_z^i and ω_0^i denote the Pauli spin operator and the transition frequency of the i^{th} qubit, respectively. For simplicity, all three qubits are taken to have the same transition frequency ω_0 . Each local environment associated with the i^{th} qubit is modeled as a collection of bosonic modes with frequencies ω_{ik} ; the operators b_{ik}^\dagger and b_{ik} are the creation and annihilation operators associated to the k^{th} mode of this local environment interacting with the i^{th} qubit, and g_{ik} characterizes the coupling strength between the i^{th} qubit and the k^{th} mode of that local environment. Initially, the three-qubit system is

assumed to be decoupled from its environment and each local environment is initially in thermal equilibrium at a temperature T_i . The subsequent dynamics generated by the total Hamiltonian H are obtained by tracing out the environmental degrees of freedom, yielding the reduced density matrix of the three-qubit system. For the tripartite system, the quantum master equation describing the decay dynamics under local dephasing is given by

$$\frac{d}{dt}\rho(t) = -\frac{i}{\hbar}[H_S, \rho(t)] + \sum_{i=1}^3 \gamma_i(t) \left(\sigma_z^i \rho(t) \sigma_z^i - \rho(t) \right), \quad (2)$$

where the system Hamiltonian is

$$H_S = \frac{\hbar}{2} \sum_{i=1}^3 \omega_0 \sigma_z^i \quad (3)$$

and the time-dependent dephasing rate is given by

$$\gamma_i(t) = 2 \int_0^\infty d\omega J_i(\omega) \coth\left(\frac{\hbar\omega}{2kT_i}\right) \frac{\sin(\omega t)}{\omega}. \quad (4)$$

Here $J_i(\omega) = \sum_k |g_{ik}|^2 \delta(\omega - \omega_{ik})$ is the spectral density of the local environment for the i^{th} qubit. In the continuum limit, the discrete mode index is replaced by a continuous frequency variable, such that $g_{ik} \rightarrow g_i(\omega)$ and the summation transforms into an integral weighted by the density of states. As a result, the spectral density can be expressed as $J_i(\omega) = P_i(\omega) |g_i(\omega)|^2$, where $P_i(\omega)$ is the density of states of the i^{th} reservoir. The time-dependent dephasing rate $\gamma_i(t)$ is fully determined by the spectral density $J_i(\omega)$. For the current model, we consider an Ohmic spectral density [45] given by

$$J_i(\omega) = \eta_i \omega \exp\left(-\frac{\omega}{\Lambda_i}\right), \quad (5)$$

where η_i represents system-reservoir coupling strength and Λ_i is the cutoff frequency. Typically, the environment is considered to be large enough to rapidly back to its initial state. Here, the impact of reservoir memory effect, encoded by $J_i(\omega)$, on the coherence dynamics of the three-qubit system is explicitly investigated. Usually, quantum master equations are derived under Markovian assumption [21, 22, 23], characterized by a bath relaxation time that is significantly shorter than the system's evolution time. In Markovian regime, memory effects in the environment are negligible. However, if the bath relaxation time becomes comparable to (or longer than) the system timescale, environmental memory effects can no longer be ignored. In such cases, the decoherence dynamics of the three-qubit system must be described using the full non-Markovian master equation in Eq. (2), which incorporates time-dependent decay rates $\gamma_i(t)$ as given in Eq. (4).

2.2. Three Qubits Under Common Dephasing Environment

Now, we consider the model where a spin-boson framework consisting of all three qubits is under the interaction with a common reservoir as shown in Fig. 1. The total Hamiltonian for the three qubits coupled to a common environment is

$$H = \frac{\hbar}{2} \sum_{i=1}^3 \omega_0^i \sigma_z^i + \sum_k \hbar \omega_k b_k^\dagger b_k + \hbar S_z \sum_k \left(g_k b_k^\dagger + g_k^* b_k \right), \quad (6)$$

where $S_z = \sum_i \sigma_z^i$ denotes the collective spin operator for the tripartite qubit system. For this model, we consider all three qubits have the same transition frequency $\omega_0^i = \omega_0$. The common environment is modelled as a set of bosonic field modes with frequencies ω_k ; the operators b_k and b_k^\dagger are the annihilation and creation operators associated with the k^{th} mode of the environment. In this model, we begin with a factorized

initial state where the system and environment are decoupled, and the common environment is in thermal equilibrium at some temperature T . For the tripartite system, the quantum master equation denotes the decay dynamics under a common dephasing environment at a finite temperature governed by

$$\frac{d}{dt}\rho(t) = -\frac{i}{\hbar}[H_S, \rho(t)] + \gamma(t)S_z\rho(t)S_z - \alpha(t)S_zS_z\rho(t) - \alpha^*(t)\rho(t)S_zS_z, \quad (7)$$

where $\gamma(t)$ is given by equation (4) with an appropriate common spectral density $J(\omega)$ and

$$\alpha(t) = \int_0^\infty d\omega J(\omega) \coth\left(\frac{\hbar\omega}{2kT}\right) \frac{\sin(\omega t)}{\omega} - i \int_0^\infty d\omega J(\omega) \frac{1 - \cos(\omega t)}{\omega}. \quad (8)$$

In this work, the temperature dependence of the coherence dynamics is investigated for non-Markovian regimes using an Ohmic spectral density $J(\omega) = \eta\omega \exp(-\omega/\Lambda)$. For numerical simulations, we vary the initial temperature of the thermal reservoir kT in unit of $\hbar\omega_0$. The other parameter values are taken as $\eta = 0.1\omega_0$, and $\Lambda = 10^{-2}\omega_0$. Next, we investigate the coherence dynamics of various tripartite initial states under both LDE and CDE. We emphasize that the dephasing rate $\gamma(t)$, given by Eq. (4), as well as the time-dependent coefficient $\alpha(t)$ appearing in the above non-Markovian master equation, explicitly depend on thermal factors. This intrinsic temperature dependence establishes a direct connection between coherence dynamics and the surrounding thermal environment. Consequently, the time-resolved decay profile of quantum coherence can be exploited as a resource for quantum thermometry. In multipartite systems, the interplay between state structure and system-environment coupling leads to distinct temperature sensitivities, resulting in state-dependent modulation of thermal decoherence. This feature is directly relevant to quantum calorimetry, where engineered quantum platforms probe microscopic energy exchange. Accordingly, analyzing coherence under thermal variations not only clarifies decoherence mechanisms but also identifies regimes in which coherence itself can serve as an effective temperature estimator in structured non-Markovian environments.

3. States subjected to non-Markov Dephasing Noise

Now we discuss the pure and mixed states that we have considered in this work for analysis.

3.1. Pure states

We now revisit the pure states, we have considered here, such as GHZ , W , $W\bar{W}$, and $Star$ states. The structural characteristics of these states are as follows.

Tripartite pure states are classified into two inequivalent categories under Stochastic Local Operations and Classical Communication (SLOCC), namely those pertaining to GHZ class and those to W class. The GHZ state shows genuine tripartite entanglement i.e. the loss of any one qubit destroys all entanglement in the system. Unlike GHZ state, the W state does not exhibit genuine tripartite entanglement. Rather, the state's entanglement is distributed in a bipartite fashion, which means, tracing out or decohering one qubit from W state does not completely eliminate entanglement among the remaining qubits. The GHZ and W states are defined as [46, 47]

$$\begin{aligned} |GHZ\rangle &= \frac{1}{\sqrt{2}}(|000\rangle + |111\rangle), \\ |W\rangle &= \frac{1}{\sqrt{3}}(|100\rangle + |010\rangle + |001\rangle). \end{aligned} \quad (9)$$

In addition, we consider two other relevant tripartite states, namely the $|W\bar{W}\rangle$ and $|Star\rangle$ states [48, 49, 50]. The $W\bar{W}$ state is constructed as an equal coherent superposition of the W state and its spin-flipped counterpart $|\bar{W}\rangle$, given by

$$|W\bar{W}\rangle = \frac{1}{\sqrt{2}}(|W\rangle + |\bar{W}\rangle), \quad (10)$$

where

$$|\overline{W}\rangle = \frac{1}{\sqrt{3}}(|011\rangle + |101\rangle + |110\rangle). \quad (11)$$

The $W\overline{W}$ state is particularly suitable for investigating coherence and correlations since it exhibits quantum coherence at single-qubit, bipartite, and tripartite levels, along with nontrivial bipartite and tripartite correlations. Thus, it serves as an effective platform for analyzing how quantum correlations are distributed across different subsystems. It is worth noting that the GHZ , W , and $W\overline{W}$ states are symmetric under permutation of qubits. Therefore, the entanglement properties of their reduced bipartite states remain invariant regardless of which qubit experiences decoherence.

The *Star* state is somewhat different from the rest. This state is asymmetric in nature and displays an uneven distribution of correlations. The *Star* state is defined as

$$|Star\rangle = \frac{1}{2}(|000\rangle + |100\rangle + |101\rangle + |111\rangle). \quad (12)$$

Similar to the $W\overline{W}$ state, the *Star* state also possesses coherence and correlations at all hierarchical levels. However, due to its asymmetric structure, it consists of two distinct types of qubits, (i) two peripheral qubits (the first and second) and (ii) one central qubit (the third). If the central qubit is traced out, the remaining two qubits become separable. Conversely, tracing out the two peripheral qubits leaves residual entanglement in the reduced state.

We examine these four tripartite pure states defined above and investigate the evolution of their coherence under dephasing dynamics and subjected to finite temperature reservoir.

3.2. Mixed states

The three mixed states that we have taken into account here are

1. $|GHZ\rangle - |W\rangle$ mixture (denoted by ρ_{GHZ}^W),
2. *Werner* - $|GHZ\rangle$ mixture (denoted by ρ_{WER}^{GHZ}),
3. *Werner* - $|W\rangle$ mixture (denoted by ρ_{WER}^W),

respectively. The mixture of the GHZ and W states, *Werner* and GHZ states, and *Werner* and W states are defined as follows:

$$\rho_{GHZ}^W = p|GHZ\rangle\langle GHZ| + (1-p)|W\rangle\langle W|, \quad (13)$$

$$\rho_{WER}^{GHZ} = p|GHZ\rangle\langle GHZ| + \frac{1-p}{8}\mathbb{I}_8, \quad (14)$$

and

$$\rho_{WER}^W = p|W\rangle\langle W| + \frac{1-p}{8}\mathbb{I}_8. \quad (15)$$

Here, p is the probability of mixing and \mathbb{I}_8 is the identity matrix of order 8. The states are defined in Eqs.(13), (14) and (15).

4. Results and Discussion

In this section we now discuss and analyze our findings.

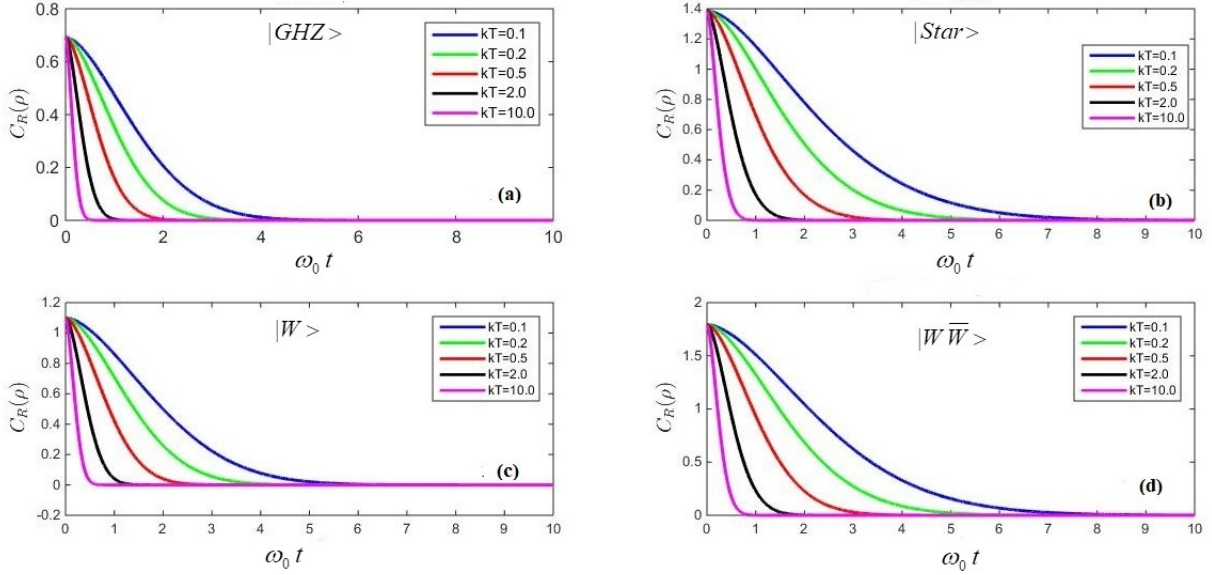


Figure 2: The dynamics of coherence of pure states in a non-Markovian local environment. Here (a) represents the relative entropy of coherence $C_R(\rho)$ for the GHZ state with dephasing strength parameter $kT = 0.1, 0.2, 0.5, 2, 10$; (b) shows the relative entropy of coherence $C_R(\rho)$ for the $Star$ state with same dephasing strength parameter while Figs. (c) and (d) are showing dynamics of $C_R(\rho)$ for W state and $W\bar{W}$ state respectively.

4.1. Pure states

We shall first analyze how the pure states defined in Eqs. (9), (10) and (12) behave in non-Markovian bath with thermal fluctuations.

4.1.1. Pure States in Local Environment

In figs.2(a), 2(b), 2(c) and 2(d), we plot the time evolution of the relative entropy of coherence $C_R(\rho)$ of the states $|GHZ\rangle$, $|Star\rangle$, $|W\rangle$ and $|W\bar{W}\rangle$ respectively, each subjected to local non-Markovian environment. Each graph 2(a) – 2(d) exhibits five curves corresponding to different values of the dephasing strength parameter kT as indicated in the legend.

In fig. 2(a) all the curves originate at the same initial coherence near $C_R(\rho) \approx 0.70$ and decay monotonically toward zero over time, whereas higher kT values exhibit markedly faster decoherence. In particular, the curve for $kT = 10$ (magenta curve) collapses to zero at very short times, while the curve corresponding to $kT = 0.1$ (blue) shows a markedly more gradual decline, maintaining non-zero coherence over a broader temporal window. The general trend demonstrates that increasing values of kT accelerate complete coherence loss in the GHZ state within this local non-Markovian dephasing framework, with no observed revivals in the plotted interval.

Fig. 2(b) presents the dynamics of coherence $C_R(\rho)$ of the $Star$ state under a local non-Markovian environment. All curves begin near maximum coherence ($C_R(\rho) \approx 1.4$) and decay monotonically toward zero as time progresses, with higher values kT leading to faster decoherence. The magenta curve ($kT = 10$) exhibits a rapid collapse, reaching zero in a short period. In contrast, the blue curve ($kT = 0.1$) retains considerable coherence throughout a wider interval compared to Fig. 2(a). No coherence revival phenomena are observed in the explored parameter regime.

Figs. 2(c) and 2(d) display the temporal dynamics of the relative entropy of coherence $C_R(\rho)$ for the $|W\rangle$ state and the $|W\bar{W}\rangle$ state exposed to a local non-Markovian environment, respectively. It can be observed

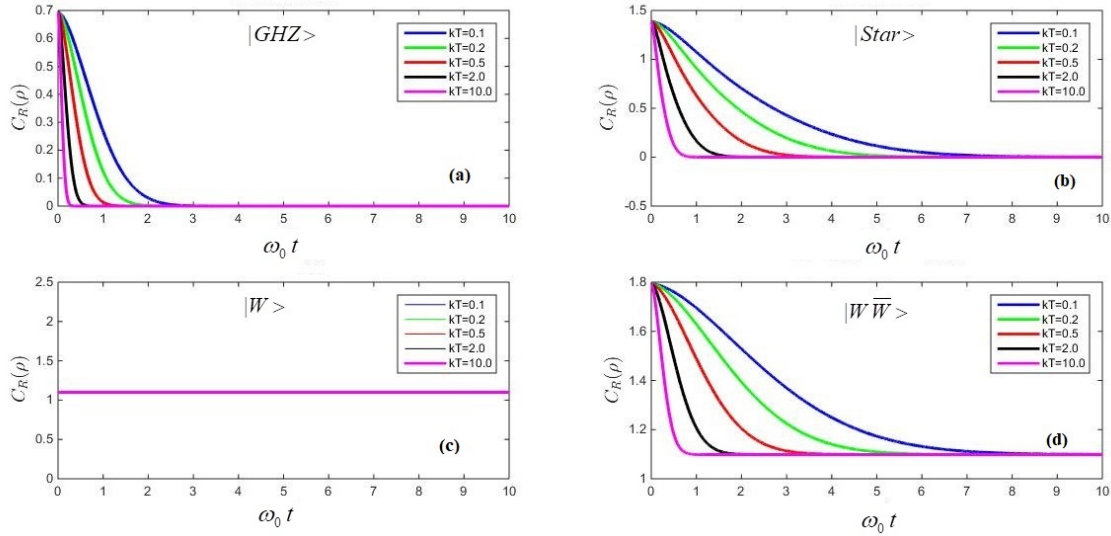


Figure 3: The dynamics of coherence of pure states in a non-Markovian common dephasing environment. Here (a) represents the relative entropy of coherence $C_R(\rho)$ for the $|GHZ\rangle$ state with dephasing strength parameter $kT = 0.1, 0.2, 0.5, 2, 10$; (b) shows the relative entropy of coherence $C_R(\rho)$ for the $|Star\rangle$ state with same dephasing strength parameter while Figs. (c) and (d) are showing dynamics of $C_R(\rho)$ for $|W\rangle$ state and $|W\bar{W}\rangle$ state respectively.

that all curves start at a high coherence value ($C_R(\rho) \approx 1.1$ for $|W\rangle$ state and $C_R(\rho) \approx 1.8$ for $|W\bar{W}\rangle$ state) and exhibit a monotonic decay toward zero. The decay patterns for Figs. 2(c) and 2(d) are similar to 2(a). Here, despite some resiliency at lower values of kT , all curves feature similar irreversible monotonic decay without revival.

Across all four pure tripartite states, the local non-Markovian environment induces a strictly monotonic decay in the relative entropy of coherence, with the rate of decoherence universally accelerating as the dephasing strength parameter kT increases. The initial coherence values, reflecting differences in state structure, suggest that $|W\rangle$ and $|Star\rangle$ states are significantly more resilient to dephasing than the $|GHZ\rangle$ state, with the $|W\bar{W}\rangle$ state exhibiting the greatest robustness under weak environmental coupling. However, at high kT values, this structural protection is quickly overwhelmed, and all states experience similarly rapid loss of coherence.

A unified view of Figs. 2(a) – 2(d) reveals a common dynamical behaviour of quantum coherence for all considered tripartite pure states subjected to a local non-Markovian dephasing environment. In every case, the relative entropy of coherence $C_R(\rho)$ decreases monotonically with time and ultimately vanishes, indicating an irreversible loss of coherence without any revival within the explored parameter regime. The temperature parameter kT plays a decisive role in governing the rate of decoherence: increasing temperature systematically accelerates the decay of coherence, reflecting the enhanced phase fluctuations induced by thermal noise in the surrounding reservoir. Despite this universal decay behaviour, the degree of robustness differs across the considered states due to their distinct internal correlation structures. In particular, the $|W\rangle$ and $|W\bar{W}\rangle$ states retain coherence for a longer duration compared to the $|GHZ\rangle$ state, indicating a greater resilience of distributed entanglement structures against local dephasing. However, this structural advantage becomes less significant at higher temperatures, where strong thermal fluctuations dominate the dynamics and drive all states toward a similarly rapid loss of coherence.

4.2. Pure States in Common Environment

In Fig. 3(a) – 3(d), we present the time evolution of the relative entropy of coherence $C_R(\rho)$ for GHZ , W , $W\bar{W}$ and $Star$ states in a common non-Markovian environment. Each curve in the graphs corresponds to a different value of the dephasing strength parameter kT as indicated in the legends.

Figure 3(a) shows the coherence dynamics of the GHZ state under non-Markovian common environment. For the GHZ state, the initial coherence $C_R(\rho)$ is approximately 0.7, and all curves exhibit a rapid monotonic decay toward zero as time increases. Higher values of kT (e.g., $kT = 10$) lead to markedly accelerated coherence loss, with near-zero coherence achieved within a short timescale. Lower values of kT (e.g., $kT = 0.1$) preserve coherence over a longer duration, but eventually decay completely. No revivals or non-monotonic behaviour are observed in the GHZ state across our observed range.

Figure 3(b) shows the coherence dynamics of the $Star$ state under non-Markovian common environment. In this scenario, coherence starts at a higher initial value of $C_R(\rho) \approx 1.4$. The decay pattern is similar with GHZ state, where all curves demonstrate a monotonic decline in $C_R(\rho)$ as $\omega_0 t$ increases, with enhanced dephasing strength (higher kT) resulting in a more rapid loss of coherence. The magenta curve ($kT = 10$) drops sharply to zero, while the blue curve ($kT = 0.1$) retains appreciable coherence for a considerably longer time. As with the GHZ state, no recoherence or revival effects are seen for the $Star$ state.

From figure 3(c), we can observe that the plot for the W state reveals a striking constancy in coherence, regardless of the kT value; all curves overlap as a single flat line at $C_R(\rho) \approx 1.1$. This indicates that, in a common non-Markovian environment, the coherence of the W state is perfectly preserved over time and is entirely insensitive to environmental dephasing within the investigated parameter regime. There are no signs of decay, revival, or any non-monotonic features.

In figure 3(d), the $W\bar{W}$ state begins at a higher initial coherence value (approximately $C_R(\rho) \approx 1.8$), but here, the coherence monotonically decreases over time with a rate that accelerates as kT increases and becomes flat at $C_R(\rho) \approx 1.1$. The magenta curve ($kT = 10$) drops sharply, while the blue curve ($kT = 0.1$) retains coherence longer before ultimately reaching the same asymptotic value as the others. Despite some resilience at lower kT , all traces demonstrate irreversible monotonic decay; no coherence revival is observed in any case.

Overall, these figures indicate that in a common non-Markovian environment, both GHZ and $Star$ states observe a strictly monotonic decay of coherence and the rate of this decay is strongly controlled by the dephasing parameter kT . Where the $Star$ state maintains a higher initial coherence and resists decoherence slightly more effectively than the GHZ state at comparable kT values, but both ultimately lose all coherence under strong dephasing conditions. In addition, the W state is fully immune to coherence loss (at least for the considered times and parameters), in sharp contrast to the $W\bar{W}$ state, which experiences tunable, irreversible decoherence controlled by environmental strength.

A unified interpretation of Figs. 3(a) – 3(d) reveals that the coherence dynamics of tripartite pure states in a common non-Markovian dephasing environment are strongly governed by the internal correlation structure of the states. In this configuration, the collective interaction with a shared reservoir produces qualitatively different behaviours compared to the local environment case. For the $|GHZ\rangle$ and $|Star\rangle$ states, the relative entropy of coherence $C_R(\rho)$ exhibits a strictly monotonic decay toward zero, with higher temperature parameters kT significantly accelerating the loss of coherence. In contrast, the $|W\rangle$ state demonstrates a remarkable robustness, where the coherence remains completely preserved and independent of the environmental temperature within the investigated parameter regime. This behaviour indicates the presence of coherence trapping induced by the symmetric distribution of excitations in the $|W\rangle$ state under collective dephasing. The $|W\bar{W}\rangle$ state displays an intermediate behaviour. Although its coherence initially decreases in a temperature dependent manner, it does not vanish completely and instead saturates to a finite stationary value. These results

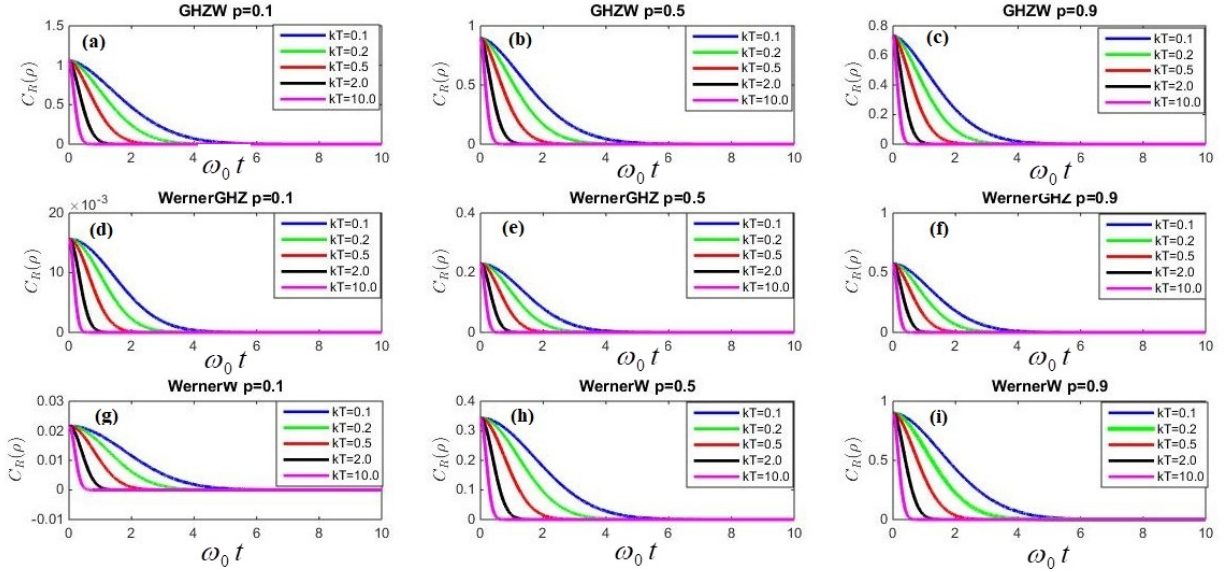


Figure 4: The dynamics of coherence of mixed states in a non-Markovian local environment. Here (a)-(c) represent the relative entropy of coherence $C_R(\rho)$ of the mixed state ρ_{GHZ}^W for mixing parameter $p = 0.1$, $p = 0.5$ and $p = 0.9$ respectively, with dephasing strength parameters $kT = 0.1, 0.2, 0.5, 2, 10$; (d)-(f) show the relative entropy of coherence $C_R(\rho)$ for the mixed state ρ_{WER}^{GHZ} with the same mixing parameters and dephasing strength parameters, while Figs. (g)-(i) show the dynamics of $C_R(\rho)$ for the mixed state ρ_{WER}^W respectively.

collectively highlight that, in a common environment, the fate of quantum coherence is not universal but is determined by the geometrical and correlation structure of the multipartite quantum state. States with distributed excitations, such as the $|W\rangle$ state, benefit from collective symmetry and exhibit strong resilience against environmental noise, whereas states with more fragile correlation structures, such as $|GHZ\rangle$, remain highly susceptible to thermal dephasing.

4.3. Mixed states

Here we focus on the mixed states defined in Eqs. (13), (14) and (15) and analyze how these states behave in non-Markovian regime along with thermal fluctuations.

4.3.1. Mixed States in Local Environment

In Fig. 4(a)–4(c), we present the dynamics of coherence $C_R(\rho)$ of the mixed state ρ_{GHZ}^W , defined in Eq. (13), in a local non-Markovian environment, for different mixing parameters p . Here, we consider three different cases $p = 0.1$, $p = 0.5$ and $p = 0.9$, respectively. Each curve in the following graphs corresponds to a different values of temperature kT . Figure 4(a), where $p = 0.1$ for ρ_{GHZ}^W , shows a decay of coherence that starts at a higher initial value $C_R(\rho) \approx 1.1$ and all curves face a rapid monotonic decay toward zero as time increases. The higher values of kT lead the curve towards accelerated complete coherence loss within a short interval ($\omega_0 t \approx 0.5$). In contrast, for lower values of kT , coherence is preserved over a comparatively longer duration but eventually decays completely. Fig. 4(b), where $p = 0.5$ for ρ_{GHZ}^W , and Fig. 4(c), where $p = 0.9$ for ρ_{GHZ}^W , the initial coherence is observed at $C_R(\rho) \approx 0.9$ and $C_R(\rho) \approx 0.7$ respectively. Otherwise, both Figs 4(b) and 4(c) illustrate characteristics similar to Fig. 4(a).

Figs. 4(d) – 4(f), represents the time evolution of quantum coherence $C_R(\rho)$ for the mixed state ρ_{WER}^{GHZ} described in Eq. (14) as a function of $\omega_0 t$ under a local non-Markovian environment. Here, we consider three different cases viz. $p = 0.1$, $p = 0.5$ and $p = 0.9$. In Fig. 4(d), where $p = 0.1$, the coherence for mixed state ρ_{WER}^{GHZ} begins at $C_R(\rho) \approx 0.015$. The coherence monotonically decreases over time with a rate that

accelerates as kT increases. When $kT = 10$ (magenta curve), the curve drops sharply, whereas for $kT = 0.1$ (blue curve), it retains coherence longer, ultimately reaching complete coherence loss. Figs. 4(e) and 4(f) show the coherence dynamics of ρ_{WER}^{GHZ} for the mixing parameter $p = 0.5$ and $p = 0.9$ respectively. In Fig. 4(e), coherence starts at an initial value $C_R(\rho) \approx 0.2$, whereas coherence starts at a higher initial value $C_R(\rho) \approx 0.6$ in Fig. 4(f). The decay patterns for both Figs 4(e) and 4(f) are similar to 4(d). Here, despite some resiliency at lower values of kT , all curves exhibit a similar irreversible monotonic decay without revival.

Figs. 4(g) – 4(i), presents the dynamical evolution of quantum coherence $C_R(\rho)$ for the mixed state ρ_{WER}^W of Eq. (15) under local non-Markovian environment. In Fig. 4(g), where $p = 0.1$, the coherence for mixed state ρ_{WER}^W begins at $C_R(\rho) \approx 0.02$. The coherence monotonically decreases over time with a rate that accelerates as kT increases. When $kT = 10$ (magenta curve), the curve drops rapidly, whereas for $kT = 0.1$ (blue curve), the curve remains coherent longer than before, ultimately reaching the complete loss of coherence. Figs. 4(h) and 4(i) show the coherence dynamics of ρ_{WER}^W for the mixing parameter $p = 0.5$ and $p = 0.9$ respectively. In Fig. 4(h), coherence starts at an initial value $C_R(\rho) \approx 0.35$, while in Fig. 4(i), it starts at a higher initial value $C_R(\rho) \approx 0.9$. The decay patterns for all curves for different values of kT in both Figs 4(e) and 4(f) are similar to those in 4(g).

A unified view of Figs. 4(a) – 4(i) reveals a consistent dynamical behaviour of quantum coherence for all the considered mixed states evolving in a local non-Markovian dephasing environment. In every case, the relative entropy of coherence $C_R(\rho)$ decreases monotonically with time and ultimately vanishes, indicating an irreversible loss of coherence without any observable revival within the explored parameter regime. The temperature parameter kT plays a decisive role in governing the decoherence dynamics: *increasing temperature systematically accelerates the decay of coherence for all the mixed states*. This behaviour reflects the enhancement of phase fluctuations induced by thermal noise in the surrounding reservoir. Although the three mixed states ρ_{GHZ}^W , ρ_{WER}^{GHZ} and ρ_{WER}^W begin with different initial coherence values depending on the mixing parameter p , the overall qualitative behaviour of their evolution remains similar. Specifically, larger values of p lead to higher initial coherence, but do not alter the fundamental decay profile. Consequently, under local non-Markovian dephasing, the dynamics of coherence for mixed states are primarily governed by environmental temperature rather than by the particular structure of the state. These observations demonstrate that the local environment acts as an efficient decohering mechanism that eventually suppresses quantum coherence in all mixed-state configurations.

4.4. Mixed States in Common Environment

In Figs. 5(a) – 5(c), we present the dynamics of coherence $C_R(\rho)$ of the mixed state ρ_{GHZ}^W of Eq. (13) under a common non-Markovian environment, for different mixing parameters p . Here, we consider three cases: $p = 0.1$, $p = 0.5$ and $p = 0.9$.

Each curve in Fig.5 corresponds to a different values of the temperature kT . Figure 5(a), where $p = 0.1$ for ρ_{GHZ}^W , shows a decay of coherence that starts at a higher initial value $C_R(\rho) \approx 1.06$ and all curves face a rapid monotonic decay toward $C_R(\rho) \approx 0.99$ as time increases. The higher values of kT lead the curve towards accelerated coherence loss in a short interval ($\omega_0 t \approx 0.1$). In contrast, for lower values of kT , coherence is preserved over a comparatively longer duration, but eventually decays to values of $C_R(\rho) \approx 0.99$. Fig. 5(b), where $p = 0.5$ for ρ_{GHZ}^W and Fig. 5(c), where $p = 0.9$ for ρ_{GHZ}^W , the initial coherence is observed at $C_R(\rho) \approx 0.9$ and $C_R(\rho) \approx 0.75$, respectively, and after a quick decay as time increases the level of coherence follows a constancy at $C_R(\rho) \approx 0.55$ and $C_R(\rho) \approx 0.15$ respectively. Otherwise, both Figs. 5(b) and 5(c) illustrate characteristics similar to Fig. 5(a).

Figs. 5(d) – 5(f), represents the dynamics of coherence $C_R(\rho)$ of the mixed state ρ_{WER}^{GHZ} of Eq. (14) under a common non-Markovian environment, for different mixing parameters p . Here, we consider three different cases $p = 0.1$, $p = 0.5$ and $p = 0.9$, respectively. Figure 5(d), where $p = 0.1$ for ρ_{WER}^{GHZ} , shows a decay of coherence that starts at a higher initial value $C_R(\rho) \approx 15$ and all curves face a rapid monotonic decay toward zero as time increases. The higher values of kT lead the curve towards accelerated complete coherence

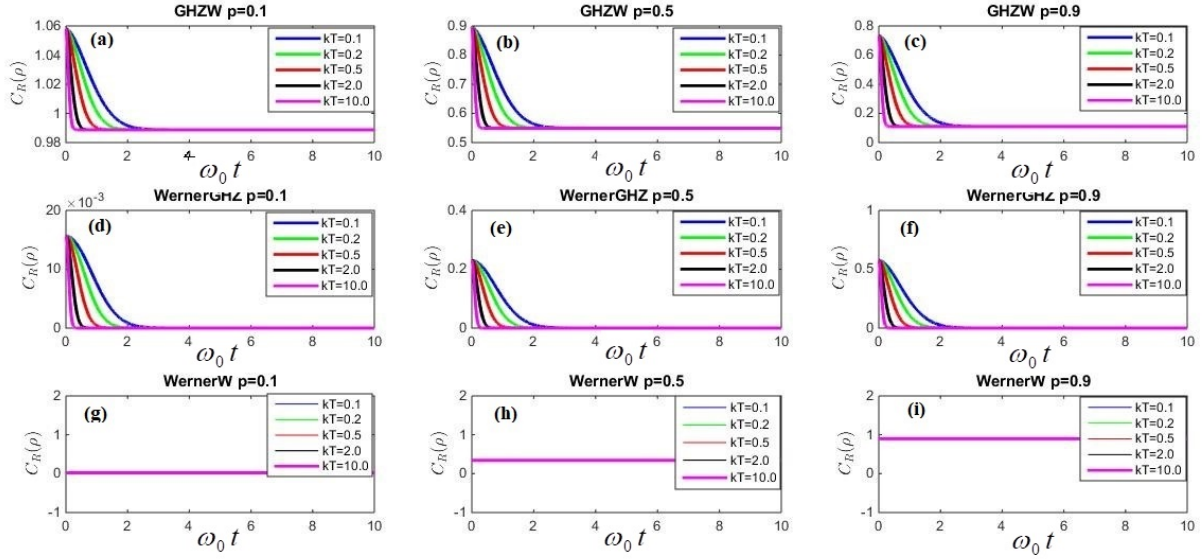


Figure 5: The dynamics of coherence of mixed states in a non-Markovian common environment. Here Figs. (a)-(c) represents the relative entropy of coherence $C_R(\rho)$ of the mixed state ρ_{GHZ}^W for mixing parameter $p = 0.1$, $p = 0.5$ and $p = 0.9$ respectively, with dephasing strength parameters $kT = 0.1, 0.2, 0.5, 2, 10$; Figs. (d)-(f) shows the relative entropy of coherence $C_R(\rho)$ for the mixed state $\rho_{WernerGHZ}^{GHZ}$ with the same mixing parameters and dephasing strength parameters, while Figs. (g)-(i) are showing dynamics of $C_R(\rho)$ for mixed state $\rho_{WernerW}^W$ respectively.

loss within a short interval ($\omega_0 t \approx 0.2$). In contrast, for lower values of kT , coherence is preserved over a comparatively longer duration but eventually decays completely. Fig. 5(e), where $p = 0.5$ for $\rho_{WernerGHZ}^{GHZ}$, and Fig. 5(f), where $p = 0.9$ for $\rho_{WernerGHZ}^{GHZ}$, the initial coherence is observed at $C_R(\rho) \approx 0.22$ and $C_R(\rho) \approx 0.5$ respectively. Otherwise, both Figs. 5(e) and 5(f) illustrate characteristics similar to Fig. 5(d).

Fig. 5(g) – 5(i), presents the dynamical evolution of quantum coherence $C_R(\rho)$ for the mixed state $\rho_{WernerW}^W$, defined in Eq. (15) under a common non-Markovian environment for different mixing parameter $p = 0.1$, $p = 0.5$ and $p = 0.9$ respectively. In Fig. 5(g), one can observe complete coherence loss for all values of kT in our investigated parameter domain. From Figs. 5(h) and 5(i), we can observe that the plot for the mixed state $\rho_{WernerW}^W$ reveals a striking constancy in coherence, regardless of kT values; all curves overlap as a single flat line at $C_R(\rho) \approx 0.3$ and $C_R(\rho) \approx 0.95$ respectively. This indicates that, in a common non-Markovian environment, the coherence of the mixed state $\rho_{WernerW}^W$ is perfectly preserved over time and is entirely insensitive to environmental dephasing within the investigated parameter regime. There are no signs of decay, revival, or any non-monotonic features.

A unified interpretation of Figs. 5(a) – 5(i) reveals that the coherence dynamics of mixed tripartite states in a common non-Markovian dephasing environment exhibit strongly state-dependent behaviour. Unlike the local environment scenario, where coherence universally decays to zero, the presence of a common reservoir leads to qualitatively different dynamical regimes depending on the internal structure of the mixed state. For the state $\rho_{WernerGHZ}^W$, the relative entropy of coherence $C_R(\rho)$ undergoes an initial rapid decay followed by saturation to a finite non-zero value, indicating the emergence of stationary coherence induced by collective system–environment coupling. In contrast, the mixed state $\rho_{WernerGHZ}^{GHZ}$ displays a strictly monotonic decay of coherence toward zero, with the rate of decoherence increasing as the temperature parameter kT grows. A markedly different behaviour is observed for the mixed state $\rho_{WernerW}^W$, where the coherence becomes completely insensitive to environmental fluctuations for certain values of the mixing parameter p , resulting in a constant

stationary coherence throughout the evolution. These results demonstrate that, in a common environment, the fate of quantum coherence is not universal but is strongly influenced by the interplay between state structure, mixing parameter, and collective environmental interactions. Consequently, certain mixed states can retain robust stationary coherence even in the presence of thermal noise, highlighting the role of state engineering in protecting quantum resources in multipartite open quantum systems.

5. Conclusion

We have investigated the coherence dynamics of multipartite quantum states in a tripartite spin boson model subjected to non-Markovian dephasing environments at finite temperature. Two distinct environmental configurations were considered, namely local and common reservoirs, and the evolution of quantum coherence was quantified using the relative entropy of coherence for both pure and mixed tripartite states. Our results show that in a local non-Markovian environment all states exhibit a universal monotonic decay of coherence, with increasing temperature accelerating the decoherence process. In contrast, the common environment produces qualitatively different behaviour depending on the structure of the quantum state. While the $|GHZ\rangle$ and $|Star\rangle$ states display complete coherence loss, the $|W\rangle$ state retains stationary coherence throughout the evolution. The $|WW\rangle$ state shows partial decay followed by saturation to a non-zero value. Similar state-dependent behaviour is also observed for mixed states. In particular, the mixed state ρ_{WER}^W demonstrates temperature-independent stationary coherence, whereas ρ_{WER}^{GHZ} undergoes complete decoherence and ρ_{GHZ}^W exhibits a finite residual coherence. These findings highlight that the thermal sensitivity of quantum coherence is strongly governed by both the reservoir structure and the internal architecture of multipartite states. The interplay between collective environmental coupling and state geometry leads to regimes ranging from rapid thermal decoherence to robust stationary coherence. Such behaviour suggests that engineered multipartite states can serve as sensitive probes of structured thermal environments, providing potential applications in coherence-based quantum thermometry and nanoscale quantum calorimetry.

Declaration of competing interest The authors declare that they have no known competing financial interests or personal relationships that could have appeared to influence the work reported in this paper.

Data availability statement All data that support the findings of this study are included within the article. No supplementary file has been added.

References

- [1] M. A. Nielsen, I. L. Chuang, Quantum computation and quantum information, Cambridge University Press, 2010.
- [2] D. Bouwmeester, A. Zeilinger, The physics of quantum information: basic concepts, quantum cryptography, quantum teleportation, quantum computation (2000) 1–14.
- [3] T. Baumgratz, M. Cramer, M. B. Plenio, Quantifying coherence, Physical Review Letters 113 (14) (2014) 140401.
- [4] A. Streltsov, G. Adesso, M. B. Plenio, Colloquium: Quantum coherence as a resource, Reviews of Modern Physics 89 (4) (2017) 041003.
- [5] R. Horodecki, P. Horodecki, M. Horodecki, K. Horodecki, Quantum entanglement, Reviews of Modern Physics 81 (2) (2009) 865–942.
- [6] C. L. Degen, F. Reinhard, P. Cappellaro, Quantum sensing, Reviews of Modern Physics 89 (3) (2017) 035002.
- [7] V. Giovannetti, S. Lloyd, L. Maccone, Advances in quantum metrology, Nature photonics 5 (4) (2011) 222–229.

- [8] H.-P. Breuer, F. Petruccione, *The theory of open quantum systems*, Oxford University Press, Oxford, 2002.
- [9] W. H. Zurek, Decoherence, einselection, and the quantum origins of the classical, *Reviews of Modern Physics* 75 (3) (2003) 715.
- [10] M. Schlosshauer, Quantum decoherence, *Physics Reports* 831 (2019) 1–57.
- [11] U. Weiss, *Quantum dissipative systems*, World Scientific, 2012.
- [12] C. H. Bennett, G. Brassard, C. Crépeau, R. Jozsa, A. Peres, W. K. Wootters, Teleporting an unknown quantum state via dual classical and einstein-podolsky-rosen channels, *Physical Review Letters* 70 (13) (1993) 1895.
- [13] R. Horodecki, M. Horodecki, P. Horodecki, Teleportation, bell’s inequalities and inseparability, *Physics Letters A* 222 (1-2) (1996) 21–25.
- [14] M. Horodecki, P. Horodecki, R. Horodecki, General teleportation channel, singlet fraction, and quasidistillation, *Physical Review A* 60 (3) (1999) 1888.
- [15] N. Gisin, G. Ribordy, W. Tittel, H. Zbinden, Quantum cryptography, *Reviews of Modern Physics* 74 (1) (2002) 145.
- [16] T. Yu, J. H. Eberly, Finite-time disentanglement via spontaneous emission, *Physical Review Letters* 93 (14) (2004) 140404.
- [17] H.-S. Goan, C.-C. Jian, P.-W. Chen, Non-markovian finite-temperature two-time correlation functions of system operators of a pure-dephasing model, *Physical Review A* 82 (1) (2010) 012111.
- [18] P.-W. Chen, M. M. Ali, Investigating leggett-garg inequality for a two level system under decoherence in a non-markovian dephasing environment, *Scientific reports* 4 (1) (2014) 6165.
- [19] C. Addis, G. Brebner, P. Haikka, S. Maniscalco, Coherence trapping and information backflow in dephasing qubits, *Physical Review A* 89 (2) (2014) 024101.
- [20] K. Berrada, A. Sabik, H. Eleuch, Quantum coherence and nonlocality of two qubits in the presence of a common dephasing environment, *Results in Physics* 51 (2023) 106666.
- [21] M. O. Scully, M. S. Zubairy, *Quantum optics*, Cambridge University Press, 1997.
- [22] H. J. Carmichael, *Statistical methods in quantum optics 1: master equations and Fokker-Planck equations*, Springer Science & Business Media, 2013.
- [23] C. Gardiner, P. Zoller, *Quantum noise: a handbook of Markovian and non-Markovian quantum stochastic methods with applications to quantum optics*, Springer Science & Business Media, 2004.
- [24] H.-P. Breuer, E.-M. Laine, J. Piilo, B. Vacchini, Colloquium: Non-markovian dynamics in open quantum systems, *Reviews of Modern Physics* 88 (2) (2016) 021002.
- [25] I. De Vega, D. Alonso, Dynamics of non-markovian open quantum systems, *Reviews of Modern Physics* 89 (1) (2017) 015001.
- [26] B. Bellomo, R. Lo Franco, G. Compagno, Non-markovian effects on the dynamics of entanglement, *Physical Review Letters* 99 (16) (2007) 160502.
- [27] F.-Q. Wang, Z.-M. Zhang, R.-S. Liang, Decoherence of two qubits in non-markovian reservoirs without the rotating-wave approximation, *Physical Review A* 78 (6) (2008) 062318.

- [28] J. Dajka, M. Mierzejewski, J. Łuczka, Non-markovian entanglement evolution of two uncoupled qubits, *Physical Review A* 77 (4) (2008) 042316.
- [29] J. P. Paz, A. J. Roncaglia, Dynamics of the entanglement between two oscillators in the same environment, *Physical Review Letters* 100 (22) (2008) 220401.
- [30] J.-G. Li, J. Zou, B. Shao, Entanglement evolution of two qubits under noisy environments, *Physical Review A* 82 (4) (2010) 042318.
- [31] D. Braun, Creation of entanglement by interaction with a common heat bath, *Physical Review Letters* 89 (27) (2002) 277901.
- [32] L. Mazzola, S. Maniscalco, J. Piilo, K.-A. Suominen, B. M. Garraway, Sudden death and sudden birth of entanglement in common structured reservoirs, *Physical Review A* 79 (4) (2009) 042302.
- [33] M. M. Ali, P.-W. Chen, H.-S. Goan, Decoherence-free subspace and disentanglement dynamics for two qubits in a common non-markovian squeezed reservoir, *Physical Review A* 82 (2) (2010) 022103.
- [34] A. Sarlette, J.-M. Raimond, M. Brune, P. Rouchon, Stabilization of nonclassical states of the radiation field in a cavity by reservoir engineering, *Physical Review Letters* 107 (1) (2011) 010402.
- [35] B.-H. Liu, L. Li, Y.-F. Huang, C.-F. Li, G.-C. Guo, E.-M. Laine, H.-P. Breuer, J. Piilo, Experimental control of the transition from markovian to non-markovian dynamics of open quantum systems, *Nature Physics* 7 (12) (2011) 931–934.
- [36] E.-M. Laine, H.-P. Breuer, J. Piilo, C.-F. Li, G.-C. Guo, Nonlocal memory effects in the dynamics of open quantum systems, *Physical Review Letters* 108 (21) (2012) 210402.
- [37] B. Bylicka, D. Chruściński, S. Maniscalco, Non-markovianity and reservoir memory of quantum channels: a quantum information theory perspective, *Scientific reports* 4 (1) (2014) 5720.
- [38] J. Nokkala, F. Galve, R. Zambrini, S. Maniscalco, J. Piilo, Complex quantum networks as structured environments: engineering and probing, *Scientific reports* 6 (1) (2016) 26861.
- [39] T. M. Stace, Quantum limits of thermometry, *Physical Review A* 82 (1) (2010) 011611.
- [40] S. Jevtic, D. Newman, T. Rudolph, T. M. Stace, Single-qubit thermometry, *Physical Review A* 91 (1) (2015) 012331.
- [41] L. A. Correa, M. Mehboudi, G. Adesso, A. Sanpera, Individual quantum probes for optimal thermometry, *Physical review letters* 114 (22) (2015) 220405.
- [42] M. Lostaglio, K. Korzekwa, D. Jennings, T. Rudolph, Quantum coherence, time-translation symmetry, and thermodynamics, *Physical review X* 5 (2) (2015) 021001.
- [43] M. G. Paris, Achieving the landau bound to precision of quantum thermometry in systems with vanishing gap, *Journal of Physics A: Mathematical and Theoretical* 49 (3) (2016) 03LT02.
- [44] A. De Pasquale, D. Rossini, R. Fazio, V. Giovannetti, Local quantum thermal susceptibility, *Nature communications* 7 (1) (2016) 12782.
- [45] A. J. Leggett, S. Chakravarty, A. T. Dorsey, M. P. Fisher, A. Garg, W. Zwerger, Dynamics of the dissipative two-state system, *Reviews of Modern Physics* 59 (1) (1987) 1.
- [46] M. Kafatos, *Bell’s theorem, quantum theory and conceptions of the universe*, Springer Science & Business Media, 2013.
- [47] W. Dür, G. Vidal, J. I. Cirac, Three qubits can be entangled in two inequivalent ways, *Physical Review A* 62 (6) (2000) 062314.

- [48] S. Roy, A. Bhattacharjee, C. Radhakrishnan, M. M. Ali, B. Ghosh, Exploring quantum properties of bipartite mixed states under coherent and incoherent basis, *International Journal of Quantum Information* 21 (02) (2023) 2350010.
- [49] H. Cao, C. Radhakrishnan, M. Su, M. M. Ali, C. Zhang, Y.-F. Huang, T. Byrnes, C.-F. Li, G.-C. Guo, Fragility of quantum correlations and coherence in a multipartite photonic system, *Physical Review A* 102 (1) (2020) 012403.
- [50] A. Bhattacharjee, A. Mandal, S. Roy, Teleportation of unknown qubit via star-type tripartite states, *Quantum Information Processing* 24 (65) (2025).